

The preceding equations are invariant with respect to representation, but for an actual calculation one must of course decide on some specific representation. For the purpose of this Appendix the exchange is most conveniently formulated as occurring in an explicit four-spin system [ABCD] defining a 16-dimensional spin Hilbert space. The mechanism M_5 can then be characterized by the two schemes

$$\text{I: } [ABCD] \rightleftharpoons [DCBA] \quad (10)$$

$$\text{II: } [ABCD] \rightleftharpoons [BADC] \quad (11)$$

contributing with statistical factors of $1/3$ and $2/3$, respectively. The exchanges are most easily described by expressing the Hilbert space permutation operators P_1' and P_{11}' in a primitive spin product basis, hereafter distinguished by primes. We then get²³

$$\mathbf{X}' = k_5(P_1' \otimes P_1'/3 + 2P_{11}' \otimes P_{11}'/3 - I) \quad (12)$$

where the symbol \otimes denotes a tensor product and I is the identity superoperator in spin Liouville space. For \mathbf{R}' we take the representation-independent phenomenological form

$$\mathbf{R}' = -I/T_1 = \mathbf{R} \quad (13)$$

which, naturally, can only be an acceptable approximation as long as relaxation does not dominate.

For specifying the deviation density vector $\eta(t)$ of eq 4 at time $t = 0$, right after an SPI by means of a DANTE pulse sequence, it is clearly more convenient to work in the eigenbasis of the static spin Hamiltonian \mathcal{H} . Referred to this eigenbasis, the equations need only be formulated in the 16-dimensional spin Liouville

subspace spanned by the diagonal elements of the density matrix. It is then trivially easy to generate $\rho(0)$ by simple interchanges of the pertinent elements (corresponding to the inverted lines) in the thermal equilibrium spin density vector, which in the present instance assumes the form

$$\rho_0^\dagger = C(-2, -1, -1, -1, -1, 0, 0, 0, 0, 0, 0, 1, 1, 1, 1, 2) \quad (14)$$

apart from an irrelevant scaling factor C . So \mathbf{X}' must be suitably transformed, which can be accomplished by a unitary supertransformation¹⁹ in spin Liouville space:

$$\mathbf{X} = \mathbf{U}^\dagger \mathbf{X}' \mathbf{U} \quad (15)$$

where

$$\mathbf{U} = \mathbf{U} \otimes \mathbf{U}^* \quad (16)$$

and

$$\mathbf{U}^\dagger \mathbf{H} \mathbf{U} = E_{\text{diag}} \quad (17)$$

Alternatively, the permutation operators may be transformed in spin Hilbert space:

$$\mathbf{P} = \mathbf{U}^\dagger \mathbf{P}' \mathbf{U} \quad (18)$$

and \mathbf{X} calculated from the unprimed equation

$$\mathbf{X} = k_5(P_1 \otimes P_1/3 + 2P_{11} \otimes P_{11}/3 - I) \quad (19)$$

Registry No. 4, 79839-45-5; 5, 79839-46-6; 6, 79839-47-7; 7, 79839-48-8; 2-bromoisophthalaldehyde, 79839-49-9; 2,6-dimethylbromobenzene, 576-22-7; 2,6-bis(difluoromethyl)bromobenzene, 79839-50-2.

Assignment of the Infrared Spectrum for the Ethyl Radical

J. Pacansky* and M. Dupuis

Contribution from IBM Research Laboratory, San Jose, California 95193.

Received March 18, 1981

Abstract: The infrared spectra of CH_3CH_2 , CH_3CD_2 , CD_3CH_2 , and CD_3CD_2 have been observed in argon matrices by photolysis of the corresponding dipropionyl peroxides. The spectra of the isotopic species coupled with detailed ab initio calculations have provided the basis for an assignment. The analysis has revealed the spectral features that are clearly a manifestation of the unpaired electron.

Although the ESR spectrum of the ethyl radical has been reported by several groups,¹⁻³ only a few studies on the optical spectra of the ethyl radical exist. The electronic absorption spectrum, observed by Hunziker and Wendt,⁴ and later by Parkes and Quinn,⁵ revealed the presence of bands at 2060 and 2460 Å; presumably, the excitations could be described as a Rydberg and a valence transition, respectively. Owing to the diffuse nature of the bands, very little structural information could be gleaned from the electronic absorption studies.

The pertinent structural data that are needed to understand chemical reactivity of radicals pertains to the ground state. Toward this end, Pacansky, Bargon, and Gardini⁶ reported the infrared spectrum of the ethyl radical. A preliminary analysis

of this spectrum revealed that the structure of the ethyl radical could be described as consisting of a methyl and methylene group much like that in ethane and ethylene. Subsequently, Pacansky and Coufal⁷ studied the deuterated species HCD_2CD_2 and concluded that the barrier for internal rotation about the C-C bond in the ethyl radical was very low or, most likely, nonexistent.

In this report, detailed experimental and theoretical studies are described on the ethyl radical in order to provide an assignment for the infrared absorptions. This assignment has provided very useful structural information for the ground state and has revealed the spectral features that are a manifestation of the unpaired electron.

Experimental Section

The various isotopically substituted dipropionyl peroxides were synthesized using the procedure developed by Johnson,⁸ where KO_2 is used to convert an acid chloride to a diacyl peroxide. The propionyl chlorides were prepared using standard procedures⁹ for converting acids to acid

(1) R. W. Fessenden and R. H. Schuler, *J. Chem. Phys.*, **39**, 2147 (1963).
 (2) J. K. Kochi and P. J. Krusic, *J. Am. Chem. Soc.*, **91**, 3940 (1969).
 (3) C. A. McDowell, P. Raghunathan, and K. Shimohoshi, *J. Chem. Phys.*, **58**, 114 (1973).
 (4) H. E. Hunziker and R. Wendt, XIth International Symposium on Free Radicals, Berchtesgaden-Königssee, Sept 4-7, 1973.
 (5) D. A. Parkes and C. P. Quinn, *J. Chem. Soc., Faraday Trans. 1*, **72**, 1952 (1976).
 (6) J. Pacansky, J. Bargon, and G. P. Gardini, *J. Am. Chem. Soc.*, **98**, 2665 (1976).

(7) J. Pacansky and H. Coufal, *J. Chem. Phys.*, **72**, 5285 (1980).

(8) R. A. Johnson, *Tetrahedron Lett.*, 331 (1976).

(9) J. D. Roberts and M. C. Caserio, "Basic Principles of Organic Chemistry", W. A. Benjamin, New York, 1964.

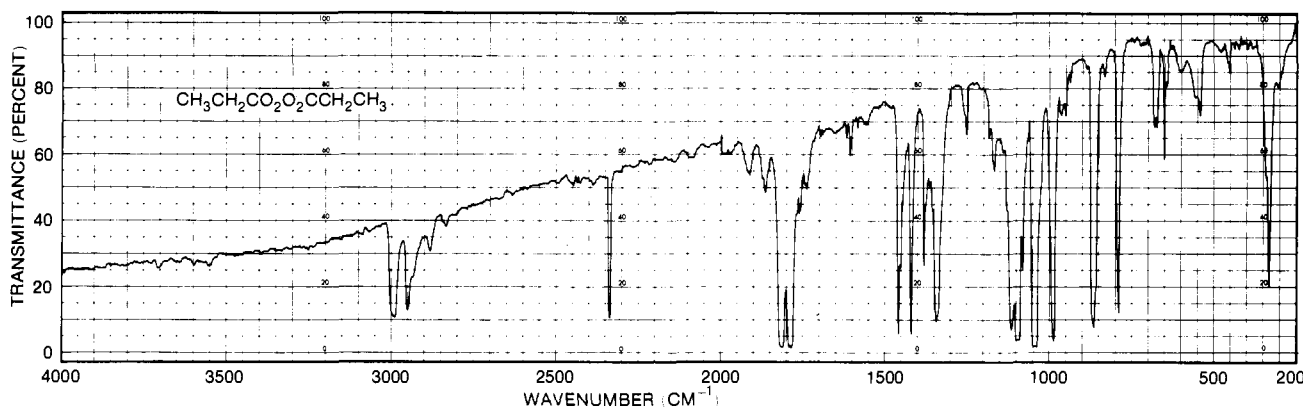


Figure 1. The infrared spectrum of dipropionyl peroxide isolated in argon ($T \approx 10$ K; concentration $\sim 1/400$).

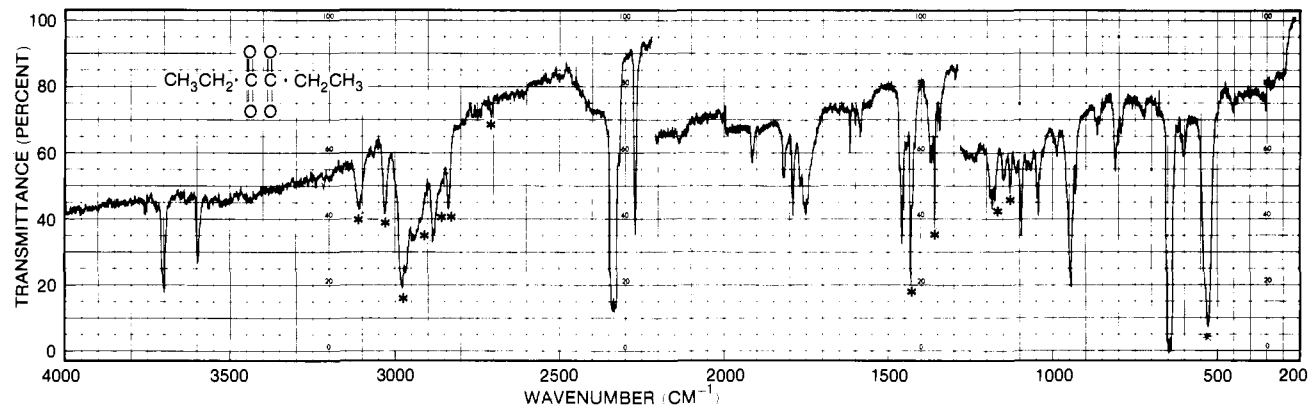


Figure 2. The infrared spectrum of dipropionyl peroxide isolated in an argon matrix after $t = 60$ h of irradiation with UV light with $\lambda > 2800$ Å.

chlorides with thionyl chloride. The propionic acid was purchased from Aldrich, and the $\text{CD}_3\text{CD}_2\text{CO}_2\text{H}$, $\text{CH}_3\text{CD}_2\text{CO}_2\text{H}$, and $\text{CD}_3\text{CH}_2\text{CO}_2\text{H}$ compounds were obtained from Merck.

The equipment used for the matrix isolation were previously reported.^{10,11} All infrared spectra were recorded using a Perkin-Elmer 621 infrared spectrometer.

Computational Details. An extensive ab initio study was reported for the structure of the ethyl radical.¹² Here, the calculations have been extended to obtain all of the vibrational modes.¹³ In addition, the computed vibrational spectrum for ethane and ethylene are included in order to calibrate the dependability of the computed normal modes for the ethyl radical.

The UHF calculations for the vibrational frequencies were performed using the program HONDO.^{14,15} The UHF calculations used the 4-31G basis set of Ditchfield et al.,¹⁶ which was found to reproduce the qualitative features obtained with a more extended basis set described in ref 12. (See also the section below describing the theoretical structure of the ethyl radical.)

Results and Discussion

Infrared Absorptions of the Ethyl Radical Observed in Argon Matrices. The infrared spectrum of dipropionyl peroxide isolated in an argon matrix at $T = 10$ K is shown in Figure 1. The infrared spectrum of dipropionyl peroxide after $t = 60$ h of irradiation with a 1500-W General Electric HBD high-pressure mercury lamp filtered through a 10-cm water filter and a Corning No. 053 filter ($\%T$ for $\lambda < 2800$ Å) is shown in Figure 2. Comparison of the carbonyl absorptions of the peroxide in Figure 1 at ≈ 1800 cm^{-1} with the absorptions in the same region in Figure 2 clearly indicates

that the UV light has almost completely decomposed the peroxide; only those for the very intense absorptions at 1820, 1790, 1090, and 1050 are still evident in the spectrum.

The infrared absorptions in Figure 2 at 2340 and 650 cm^{-1} have been assigned to the asymmetric stretching and the bending mode of CO_2 .¹⁷ The intense band at 2270 cm^{-1} is the asymmetric stretching mode of $^{13}\text{CO}_2$. The bands at 3700 and 3600 cm^{-1} are due to various combination bands of CO_2 . All of these bands have been confirmed to be attributed to CO_2 by comparison with a spectrum of only CO_2 isolated in an argon matrix.

Another absorption prominent in the spectrum of photodecomposed peroxide is the band at 950 cm^{-1} which was shown to be due to the out-of-plane bending mode of ethylene¹⁷ by comparison with the infrared spectrum of an authentic sample of ethylene isolated in an argon matrix. That ethylene is present in this spectrum is reasonable because it was shown that the two CO_2 molecules are not 100% efficient at keeping the photochemically formed ethyl radicals apart.⁷ Ethylene, along with ethane and butane, are disproportionation and combination products of the ethyl radical. Ethane and butane are also present in this spectrum but their absorptions are not as prominent as the very intense bending mode of ethylene at 950 cm^{-1} .

The bands marked with an asterisk in Figure 2 are assigned to CH_3CH_2 on the following basis: they all appear in concert with the disappearance of dipropionyl peroxide by the action of UV light; they do not correspond to any absorptions for carbon dioxide, ethylene, ethane, or butane; and most of all the labeled bands synchronously disappear with the appearance of the absorptions due to the combination-disproportionation products of the ethyl radical when the temperature of the matrix is raised to ~ 30 K for $t = 5$ min. The spectrum after the brief warmup of the argon matrix is shown in Figure 3. This spectrum has been shown to be due only to CO_2 and the combination-disproportionation products of the ethyl radical: ethylene, ethane, and butane. In

(10) J. Pacansky, D. E. Horne, G. P. Gardini, and J. Bargon, *J. Phys. Chem.*, **81**, 2149 (1977).

(11) J. Pacansky, *J. Phys. Chem.*, **81**, 2240 (1977).

(12) J. Pacansky and M. Dupuis, *J. Chem. Phys.*, **68**, 4276 (1978).

(13) J. W. McIver and A. Komornicki, *J. Am. Chem. Soc.*, **94**, 2625 (1972).

(14) M. Dupuis, J. Rys, and H. F. King, *J. Chem. Phys.*, **65**, 111 (1976).

(15) M. Dupuis and H. F. King, *J. Chem. Phys.*, **68**, 3998 (1978).

(16) R. Ditchfield, W. J. Hehre, and J. A. Pople, *J. Chem. Phys.*, **54**, 724 (1971).

(17) G. Herzberg, "Infrared and Raman Spectra", D. Van Nostrand, Princeton, N.J., 1966.

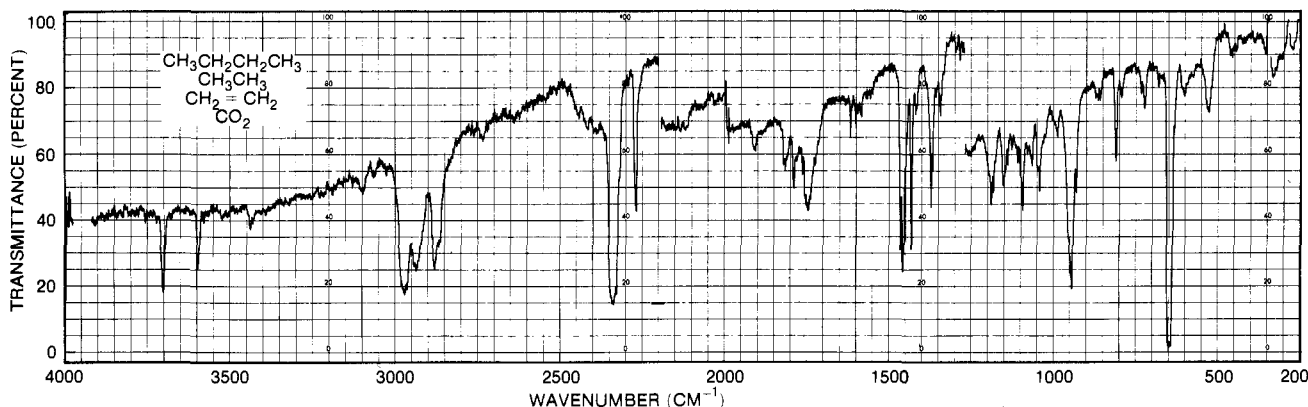


Figure 3. The infrared spectrum recorded after warming the argon matrix to $T \sim 30$ K. The spectrum was recorded at $T \sim 10$ K.

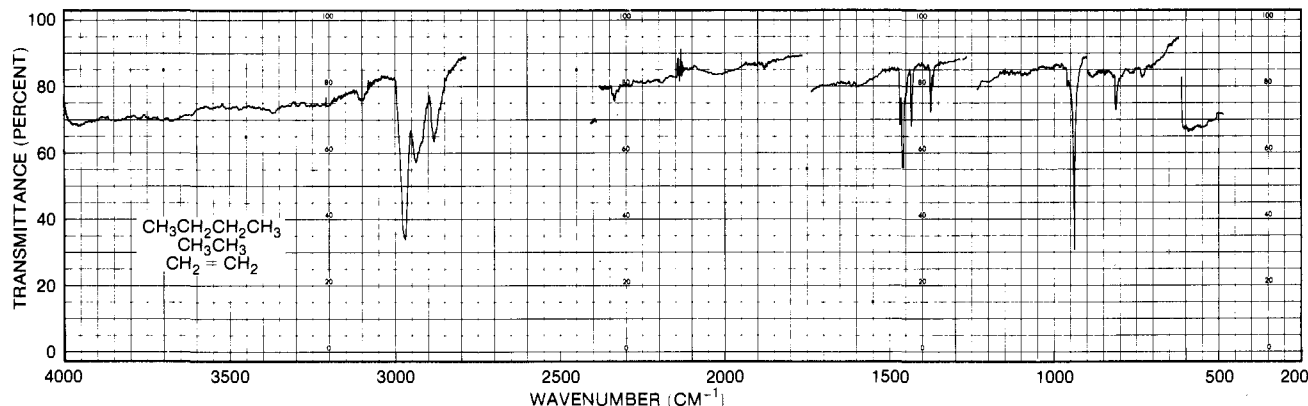


Figure 4. The infrared spectrum of an equimolar mixture of ethane, ethylene, and butane in an argon matrix.

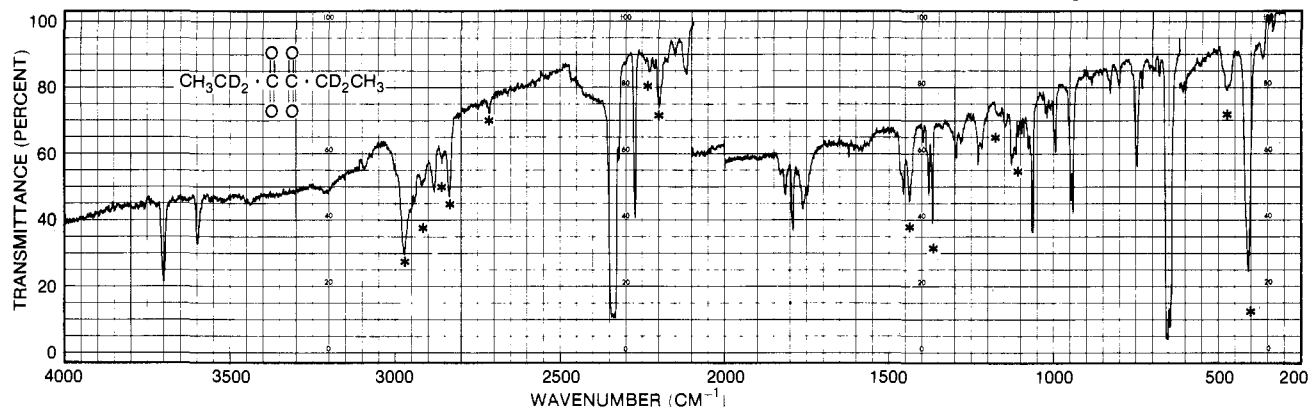


Figure 5. The infrared spectrum of CH_3CD_2 in an argon matrix obtained by irradiation of $\text{CH}_3\text{CD}_2\text{CO}_2\text{O}_2\text{CCD}_2\text{CH}_3$ with UV light ($\lambda > 2800 \text{ \AA}$) for $t = 60$ h.

order to demonstrate this further, an infrared spectrum of equal concentrations of ethylene, ethane, and butane, isolated in an argon matrix, is shown in Figure 4.

In order to identify which of the absorptions of the ethyl radical shown in Figure 2, and listed in Table I, are vibrational modes associated with the methyl (CH_3) or methylene group (CH_2), several isotopically labeled species were prepared. The infrared spectrum of the $\text{CH}_3\text{CD}_2\text{CO}_2\text{O}_2\text{CCD}_2\text{CH}_3$ peroxide isolated in argon matrix is shown in Figure 5 after conversion to CH_3CD_2 and CO_2 under identical conditions for CH_3CH_2 radical formation (Figures 1 and 2). The bands marked with an asterisk in Figure 5, and listed in Table I, have been assigned to the CH_3CD_2 radical using the same criteria used for CH_3CH_2 . By comparison of the spectra shown in Figures 2 and 5, it is very easy to identify the intense spectral features that must be assigned to the radical center, i.e., the $-\text{CH}_2$ group. The bands at 3112 , 3033 , and 540 cm^{-1} for CH_3CH_2 are shifted dramatically upon isotopic substitution to 2232 , 2201 , and 413 cm^{-1} for CH_3CD_2 . These bands must be assigned to the stretching motions of the olefinic like, α CH bonds

Table I. Observed Frequencies (cm^{-1}) for the Ethyl Radical

		CH_3CH_2	CH_3CD_2	CD_3CH_2	CD_3CD_2
methylene group	stretching	3112	2232	3124	2249
		3033	2201	3042	2199
	bending	540	413	510	398
		2987	2974	2167	2170
		2920	2920	2098	2094
methyl group	stretching	2853	2859	2045	2048
		2842	2837		
	bending	(2715)	(2715)		
		1440	1439	1039	1041
		1366	1364		1035
		1175	1166	1135	1070
		1138	1116		
			(474)		(465)

and the pyramidal like bending mode of the radical center.

Further evidence for this assignment was obtained by preparing the CD_3CH_2 radical in an argon matrix from the $\text{CD}_3\text{CH}_2\text{C}$

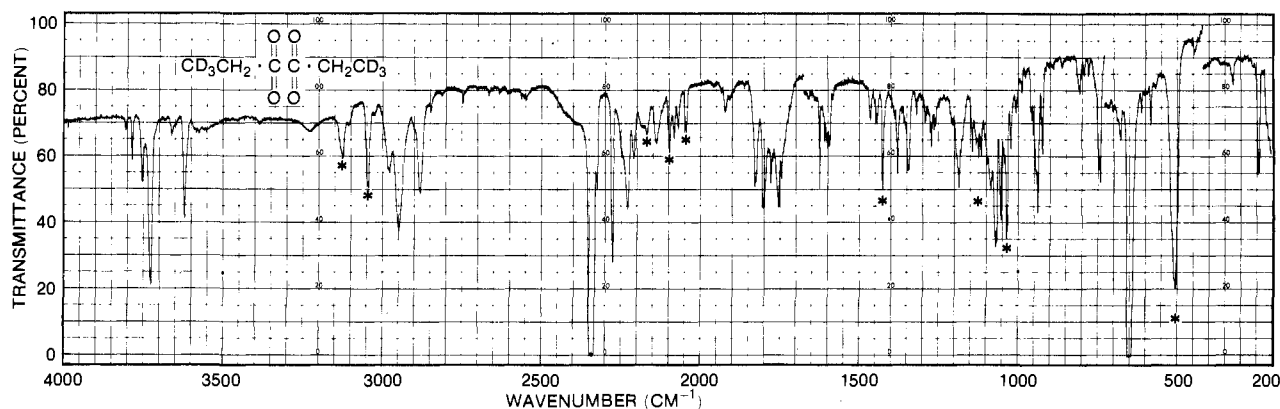


Figure 6. The infrared spectrum of CD_3CH_2 isolated in an argon matrix obtained by irradiation of $\text{CD}_3\text{CH}_2\text{CO}_2\text{O}_2\text{CCH}_2\text{CD}_3$ with UV light ($\lambda > 2800 \text{ \AA}$) for $t = 60 \text{ h}$.

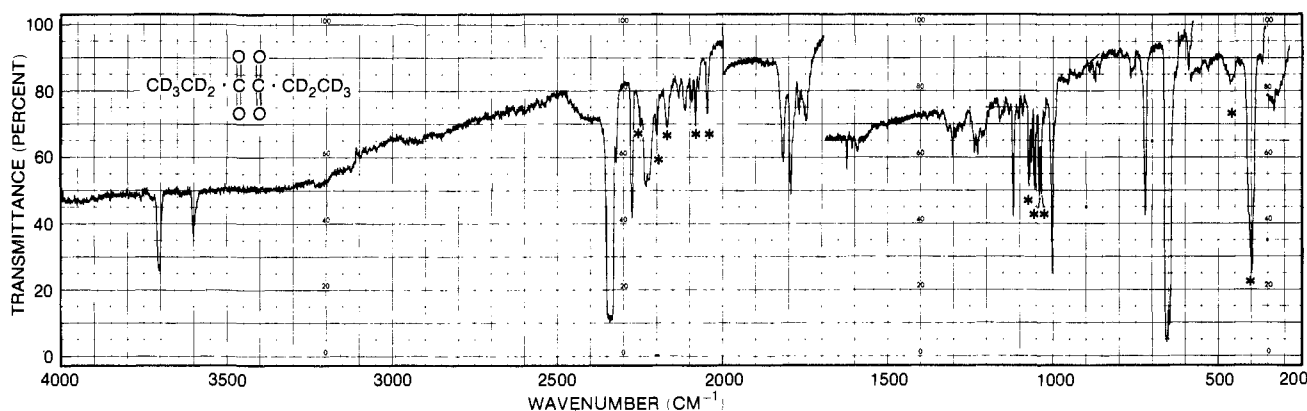


Figure 7. The infrared spectrum of CD_3CD_2 isolated in an argon matrix obtained by irradiation of $\text{CD}_3\text{CD}_2\text{CO}_2\text{O}_2\text{CCD}_2\text{CD}_3$ with UV light ($\lambda > 2800 \text{ \AA}$) for $t = 60 \text{ h}$.

$\text{O}_2\text{O}_2\text{CCH}_2\text{CD}_3$ peroxide. In Figure 6, the spectrum is shown after conversion of the peroxide to CD_3CH_2 and CO_2 . The bands marked in Figure 6 and listed in Table I have been assigned to the CD_3CH_2 radical. The most noticeable feature about the CD_3CH_2 spectrum in Figure 6 is that the region between 3000 and 2800 cm^{-1} contains several bands. This is contrary to what one would expect because upon deuteration of the methyl group all of the bands in the methyl, etc., CH stretching region should shift to lower frequency. The explanation for this is straightforward; as briefly discussed above, the CO_2 molecules are less than 100% efficient at separating the CD_3CH_2 radicals, and as a consequence some combination-disproportionation of the radicals occurs. This was readily shown to be the case by allowing combination-disproportionation of the radicals when the matrix temperature was elevated to $T \sim 30 \text{ K}$. Under these conditions, it was observed that the intensities of the bands between 3000 and 2800 cm^{-1} were increased while those bands marked with an asterisk decreased, thus unequivocally demonstrating that the bands between 3000 and 2800 cm^{-1} in Figure 6 are from combination-disproportionation products.

A comparison of the spectrum for CH_3CH_2 in Figure 2 with that for CD_3CH_2 in Figure 6 shows that the absorption assigned to the CH_2 groups in CH_3CH_2 (3112, 3033, 540 cm^{-1}) are only slightly shifted from those in CD_3CH_2 (3124, 3024, 510 cm^{-1}). The new features in the CD_3CH_2 system at 2167, 2098, and 2045 cm^{-1} are due to the stretching motions of the deuterated methyl group.

The assignment of all the frequencies which shift upon deuteration of the methyl and methylene groups, respectively, is supported by the spectrum of CD_3CD_2 . In Figure 7, the infrared spectrum of CD_3CD_2 is shown. The bands assigned to this system are marked with an asterisk in Figure 7 and are listed in Table I. It is interesting to note that the infrared spectrum of CD_3CD_2 may easily be extracted from the spectra of CD_3CH_2 and CH_3CD_2 . This is demonstrated in Table I.

Thus far the discussion on the infrared spectrum of the ethyl radical has been limited to only the stretching and the pyramidal bending modes. The reason for this is that they are intense and easy to assign, and demonstrate which group of bands are due to either the methyl or methylene group in the ethyl radical. There are other absorptions that shift along with the easily identifiable features and are assigned on this and the basis that hydrocarbons, like most systems, have characteristic infrared absorptions.¹⁸ Internal bending modes for methyl groups in hydrocarbons are observed from about 1440 to 1380 cm^{-1} . Absorptions are observed at 1440 and 1366 cm^{-1} for CH_3CH_2 and at 1439 and 1364 cm^{-1} for CH_3CD_2 . It is reasonable to assign the absorptions to the internal bending modes of the methyl group on the basis that they are associated with the CH_3 group and that they are characteristically observed in this region. Along similar lines, the bands at 1039 for CD_3CH_2 , and 1041 and 1033 for CD_3CD_2 are assigned to the internal deformation modes of the CD_3 group.

An absorption is observed at 1438 cm^{-1} for CD_3CH_2 which must be assigned to a mode in the CH_2 group. Since this frequency is rather high, a reasonable assignment is an internal bending motion of the CH_2 group. Olefins characteristically have a band in this region.¹⁸ It is somewhat disconcerting that this band was not observed in the CH_3CH_2 system, but the $\sim 1450\text{-cm}^{-1}$ region in this species has an intense absorption in which this mode could certainly be buried.

The remaining observed bands at 1175 and 1138 cm^{-1} in the CH_3CH_2 species could be assigned to either the CC stretching or rocking motions of the CH_3 group. The preferred assignment is that the 1175- cm^{-1} feature is a methyl rocking mode. The CC stretching mode should not be shifted too much by deuteration. Since bands are observed at 1166, 1135, and 1070 cm^{-1} for the CH_3CD_2 , CD_3CH_2 , and CD_3CD_2 systems, respectively, then this

(18) L. M. Sverdlov, M. A. Kovner, and E. P. Krainov, "Vibrational Spectra of Polyatomic Molecules", Wiley, New York, 1974.

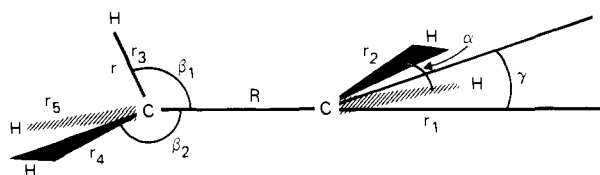


Figure 8. The optimized geometry of the ethyl radical computed using ab initio SCF calculations: $r_1 = r_2 = 1.076 \text{ \AA}$, $r_3 = 1.090 \text{ \AA}$, $r_4 = r_5 = 1.086 \text{ \AA}$, $R = 1.498 \text{ \AA}$, $\alpha = 118.38^\circ$, $\beta_1 = 112.01^\circ$, $\beta_2 = 111.42^\circ$, $\gamma = 6.19^\circ$.

Table II. Comparison of the Experimental and the Theoretical Vibrational Frequencies (cm^{-1}) for Ethane

vibrational mode	obsd	harmonic	calcd ^a
$\nu_{10}(E_g)$, asymmetric CH stretch	2950	3175	3253
$\nu_7(E_u)$, asymmetric CH stretch	2995	3140	3225
$\nu_5(A_{2u})$, symmetric CH stretch	2954	3061	3175
$\nu_1(A_{1g})$, symmetric CH stretch	2954	3043	3182
$\nu_{11}(E_g)$, asymmetric CH_3 deformation	1486	1552	1670
$\nu_8(E_u)$, asymmetric CH_3 deformation	1486	1526	1666
$\nu_2(A_{1g})$, symmetric CH_3 deformation	1388	1449	1585
$\nu_6(A_{2u})$, symmetric CH_3 deformation	1379	1438	1588
$\nu_{12}(E_g)$, CH_3 rock	1190	1246	1359
$\nu_3(A_{1g})$, C-C stretch	1016	995	1046
$\nu_9(E_u)$, CH_3 rock	822	822	924
$\nu_4(A_{1u})$, CH_3 torsion	280	303	315

^a Calculated with the 4-31G basis set.

supports this assignment. The absorption at 1138 and 1116 cm^{-1} for CH_3CH_2 and CH_3CD_2 is most likely a methyl rocking mode because upon deuteration of the methyl group this band is not observed in this region.

There are several other absorptions whose assignment is not known. They are the group of weak bands at 2715 cm^{-1} for CH_3CH_2 and CH_3CD_2 and the bands at 474 and 465 cm^{-1} for CH_3CD_2 and CD_3CD_2 , respectively.

Theoretical Structure of the Ethyl Radical. The details of the ab initio calculation for the structure of the ethyl radical was previously reported.¹² Since the structure is essential for this report, it is shown in Figure 8. The salient features of the structure that should be stressed are the following.

(1) The α CC and CH bonds are shorter than normal CH and CC bonds. While the CC bond is slightly shorter than a normal CC bond, the α CH bonds have lengths like those for ethylene.

(2) The β CH bond, r_3 , that is eclipsed with the radical center is slightly longer than the other β CH bonds. This has been consistently found for alkyl radicals with eclipsed β CH bonds.^{12,19}

(3) The radical center is nonplanar, γ , the angle between CC axis and the plane formed by the CH_2 group, is 6.19° . Consequently, the unpaired electron has steric requirements and, as a consequence, the system takes on the staggered ethane-like geometry.

Theoretical Vibrational Frequencies for Ethane, Ethylene, and the Ethyl Radical. Ab initio SCF calculations have been very useful for understanding the structure of alkyl radicals.^{12,19} Moreover, vibrational frequencies computed using the same SCF methods also appear to be a valuable aid in the assignment of experimental frequencies. Here, it is demonstrated that the theoretical infrared spectrum for ethane and ethylene appears in the same order as found experimentally. The calculated frequencies, however, are higher than the experimental frequencies, but this is not a problem since the ordering is generally correct.

The theoretical vibrational frequencies of ethane and ethylene are presented here in order to provide insight into and "calibrate" the computed infrared spectrum of the ethyl radical. This is a useful exercise because one might expect that the vibrational spectrum of the ethyl radical may be synthesized by using the appropriate frequencies for a CH_3 group in ethane with those from

Table III. Comparison of the Experimental and the Theoretical Vibrational Frequencies (cm^{-1}) for Ethylene

vibrational mode	obsd	calcd ^a
asymmetric CH stretch	3106	3405
asymmetric CH stretch	3103	3375
symmetric CH stretch	3026	3328
symmetric CH stretch	2989	3303
C=C stretch	1623	1856
CH_2 in-plane bend	1444	1639
CH_2 in-plane bend	1342	1521
CH_2 in-plane bend	1222	1386
CH_2 torsion	1024	1168
CH_2 out-of-plane	949	1126
CH_2 out-of-plane bend	943	1163
CH_2 in-plane bend	826	935

^a Calculated with the 4-31G basis set.

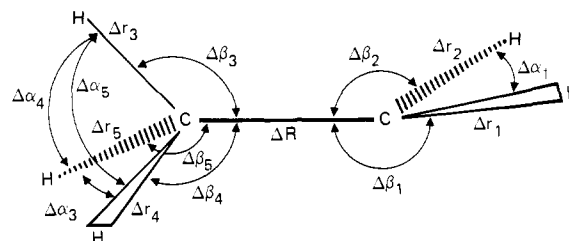


Figure 9. The internal coordinates for the ethyl radical.

a CH_2 group in ethylene. For the most part, this is the case, but there are important differences which are a manifestation of the radical center; these will be pointed out.

The computed vibrational frequencies for ethane are shown in Table II along with the observed frequencies¹⁸ with and without corrections for anharmonicity. The frequencies are listed in Table II from the highest to lowest in order to demonstrate the agreement between the experimental and theoretical ordering of the frequencies. The pertinent comparison to make is with the computed and harmonic frequencies because the former were determined within the usual harmonic oscillator approximation.

In Table III, the experimental¹⁸ and calculated frequencies are presented for ethylene where again there is good agreement between the ordering of the experimental and observed frequencies.

The computed vibrational frequencies for the ethyl radical were determined using the structure with C_s symmetry illustrated in Figure 8. The theoretical frequencies are listed in Table IV for CH_3CH_2 , CD_3CH_2 , CH_3CD_2 , and CD_3CD_2 with their assignments. The internal coordinates used to describe the vibrational modes are shown in Figure 9.

A comparison of the calculated vibrational modes of ethylene with those associated with the CH_2 group in the ethyl radical reveals that both systems are almost identical. The pertinent modes in ethylene are the CH stretches which range from 3400 to 3300 cm^{-1} , the CH_2 in-plane bends at 1639 and 935 cm^{-1} , and the CH_2 out-of-plane bend at 1126 cm^{-1} . The corresponding vibrational modes in the ethyl radical are calculated at 3397, 3294, 1608, 897, and 499 cm^{-1} . Consequently, as far as the vibrational frequencies are concerned, the methylene group in the ethyl radical is almost identical with the methylene group in ethylene with the important exception that the out-of-plane bending mode at 1126 cm^{-1} for ethylene drops to 499 cm^{-1} for the ethyl radical. This directly reflects the dramatic consequences of losing the π bond in ethylene; the methylene group, i.e., the radical center, undergoes an out-of-plane distortion requiring much smaller changes in energy than for ethylene (since the geometry about the radical center in the ethyl radical is slightly nonplanar it is better to describe the "out-of-plane bending mode" as a pyramidal bending mode).

Inspection of the calculated vibrational frequencies for a CH_3 group in ethane and comparison with those for the CH_3 group in the ethyl radical also reveal important differences created by the presence of the unpaired electron. The pertinent vibrational modes are the average of the asymmetric and symmetric CH

(19) J. Pacansky and M. Dupuis, *J. Chem. Phys.*, **71**, 2095 (1979); M. Yoshimine and J. Pacansky, *ibid.*, **74**, 5168 (1981).

Table IV. Vibrational Frequencies (cm⁻¹) for the Ethyl Radical Computed Using ab Initio Calculations^a

assignment	CH ₃ CH ₂	CD ₃ CH ₂	CH ₃ CD ₂	CD ₃ CD ₂
CH ₂ asymmetric stretch (A'')	3397	3396	2532	2532
CH ₂ symmetric stretch (A')	3294	3294	2386	2387
CH ₃ asymmetric stretch (A'')	3240	2401	3242	2400
CH ₃ symmetric stretch (A')	3206	2361	3206	2361
CH ₃ symmetric stretch (A'')	3138	2263	3138	2262
CH ₃ internal bend (A'')	1654	1190	1654	1193
CH ₃ internal bend (A')	1651	1190	1650	1189
CH ₂ bend (A')	1608	1607	1247	1279
CH ₃ internal bend (A')	1583	1253	1585	1197
CH ₃ rocking (A'')	1327	1212	1248	1064
CH ₃ rocking (A')	1120	874	1118	871
C-C stretch (A')	1096	1020	1010	957
CH ₂ asymmetric bend (A'')	897	753	728	647
CH ₂ pyramidal distortion (A')	499	490	391	383
torsion (A'')	141	126	118	100

^a Calculated with the 4-31G basis set.Table V. Assignment for the Observed Vibrational Frequencies (cm⁻¹) of the Ethyl Radical

symmetry	symmetry coordinate	description		CH ₃ CH ₂	CH ₃ CD ₂	CD ₃ CH ₂	CD ₃ CD ₂
A'	$S_1 = (\Delta r_1 + \Delta r_2)/\sqrt{2}$	CH ₂ symmetric stretch	ν_1	3033	2201	3042	2199
	$S_2 = (\Delta r_3 + \Delta r_4 + \Delta r_5)/\sqrt{3}$	CH ₃ symmetric stretch	ν_2	2920	2920	2098	2098
	$S_3 = (2\Delta r_3 - \Delta r_4 - \Delta r_5)/\sqrt{6}$	CH ₃ symmetric stretch	ν_3	2842	2837	2045	2048
	$S_4 = (2\Delta\alpha_1 - \Delta\beta_1 - \Delta\beta_2)/\sqrt{6}$	χ scissor	ν_4			1438	
	$S_5 = (2\Delta\alpha_3 - \Delta\alpha_4 - \Delta\alpha_5)/\sqrt{6}$	CH ₃ internal bend	ν_5	1440	1439	1039	1041
	$S_6 = (\Delta\alpha_3 + \Delta\alpha_4 + \Delta\alpha_5 - \Delta\beta_3 - \Delta\beta_4 - \Delta\beta_5)/\sqrt{6}$	CH ₃ internal bend	ν_6	1366	1364		1035
	$S_7 = \Delta R$	CC stretch	ν_7	1175	1166	1135	1070
	$S_8 = (2\Delta\beta_3 - \Delta\beta_4 - \Delta\beta_5)/\sqrt{6}$	CH ₃ rocking	ν_8	1138			
	$S_9 = (\Delta\alpha_1 + \Delta\beta_1 + \Delta\beta_2)/\sqrt{3}$	CH ₂ pyramidal distortion	ν_9	540	413	510	398
A''	$S_{10} = (\Delta r_1 - \Delta r_2)/\sqrt{2}$	CH ₂ asymmetric stretch	ν_{10}	3112	2232	3124	2249
	$S_{11} = (\Delta r_4 - \Delta r_5)/\sqrt{2}$	CH ₃ asymmetric stretch	ν_{10}	2987	2974	2167	2170
	$S_{12} = (\Delta\alpha_4 - \Delta\alpha_5)/\sqrt{2}$	CH ₃ internal bend	ν_{12}	1440	1439	1039	1041
	$S_{13} = (\Delta\beta_4 - \Delta\beta_5)$	CH ₃ rocking	ν_{13}		1116		
	$S_{14} = (\Delta\beta_1 - \Delta\beta_2)/\sqrt{2}$	CH ₂ asymmetric bend	ν_{14}				
	$S_{15} = \Delta\tau$	torsion	ν_{15}				

stretches at 3239, 3179 cm⁻¹, the average of the asymmetric and symmetric internal bending modes at 1668 and 1587 cm⁻¹, the two rocking modes at 1359 and 924 cm⁻¹, and the torsion mode at 315 cm⁻¹. Owing to the different symmetry of the ethyl radical three CH stretching frequencies are computed for the methyl group. The two higher ones at 3240 and 3206 are not unusual and are due to the internal coordinates Δr_4 and Δr_5 (see Figure 9). The frequency at 3138 cm⁻¹, however, is anomalous because it is lower than that normally found for a CH stretching frequency for methyl groups in alkanes. Studies on alkyl radicals have consistently shown that when β CH bonds are eclipsed with the C_{2p} orbital containing the unpaired electron, a longer than normal CH bond is found which manifests itself in the infrared by a low-frequency CH stretch.

The frequencies for the internal deformation modes of the ethyl radical at 1654, 1651, and 1583 cm⁻¹ are nominally about the same as that found in ethane. This is not the case, however, for the rocking modes. The description of the normal modes for the motions of the atoms involved in the rocking vibrations of ethane show that the nuclei are moving toward each other at the higher frequency (1359 cm⁻¹) and away from each other at the lower frequency (924 cm⁻¹). This is reversed for the ethyl radical. The frequency at 1327 cm⁻¹ corresponds to the rocking motion, described by an A'' symmetry coordinate shown in Table IV, which has the nuclei moving away from each other like that for the rocking motion in ethane at 924 cm⁻¹. The probable reason for the increase in the vibrational frequency is shown by the isotope dependence in Table IV. The deuteration of either the methyl or methylene group in the ethyl radical produces about the same shift in frequency; consequently, the mode involves a considerable mixing between motions on both the methyl and methylene groups (the calculated eigenvector for this frequency amply verifies this) and is the net result of an sp² center moving against an sp³ center.

The isotope dependence (Table IV) and the calculated eigenvector for the frequency of the rocking motion at 1120 cm⁻¹ in the ethyl radical reveals that this mode is localized on the methyl

group. The rather dramatic drop in this frequency, compared with that for ethane may conveniently be explained by the decrease in repulsive interactions created by the one less hydrogen in the ethyl radical and/or the relative ease with which the radical center (CH₂ group) distorts pyramidally. Certainly, as the hydrogen at the end of the β CH bond moves toward the radical center, repulsive interactions would be decreased if the radical readily distorts away from the approaching hydrogen nucleus.

The torsion modes are computed to be at 315 cm⁻¹ for ethane and at a much lower frequency (141 cm⁻¹) for the ethyl radical. Very little significance is attached to the calculated torsional frequencies because of numerical problems usually encountered in the computation of frequencies this low. However, the calculation does bear out that the much lower torsional frequency in the ethyl radical is an indication that a very low barrier exists for internal rotation about the CC bond in the ethyl radical.

The last vibrational mode of the ethyl radical that must be aired is the CC stretch calculated at 1096 cm⁻¹. This is slightly higher than the CC stretch in ethane computed to be at 1046 cm⁻¹. The increase in the CC stretching frequency is expected because the CC bond length is slightly shorter in the ethyl radical than a normal CC bond.

Assignment for the Observed Infrared Absorptions of the Ethyl Radical. The isotopic studies on the ethyl radical made it possible to associate a number of frequencies to either the methyl or methylene group in the ethyl radical. The theoretically determined vibrational frequencies enabled this to be more specific and comprehensive. Here, the results of the isotopic and theoretical studies are used to propose a complete assignment for all of the vibrational frequencies of the ethyl radical.

The structure of the ethyl radical used for the assignment has the C_s symmetry shown in Figure 8. The internal coordinates are defined in Figure 9; the symmetry coordinates are listed in Table V along with the assignment of all the vibrational frequencies. Since most of the reasons for this particular assignment have been discussed, then only those vibrational modes which are a mani-

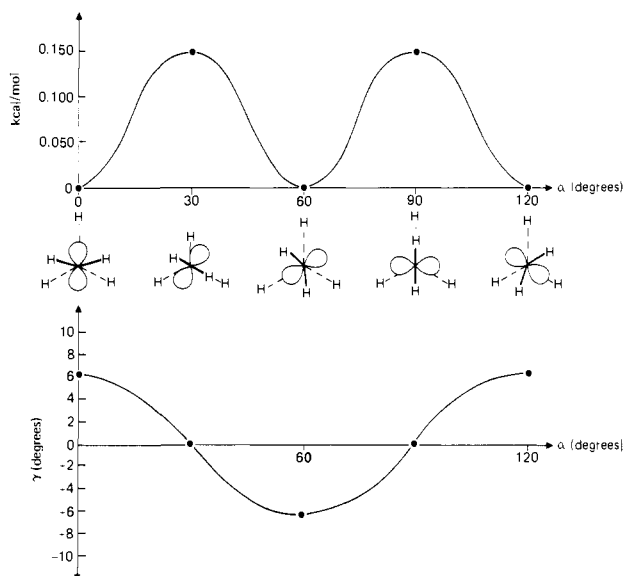


Figure 10. The potential function for internal rotation about the CC bond in the ethyl radical, and a plot of the angle γ (which is a measure of the degree of pyramidal distortion about the radical center) as a function of rotation about the CC bond. α is the angle of rotation about the CC bond; γ is the angle between the plane formed by the CH_2 group and the CC bond; both α and γ are expressed in degrees; the energy is in kcal/mol.

festation of the unpaired electron are mentioned. ν_3 , the low-frequency CH stretch at 2842 cm^{-1} , and ν_9 , the pyramidal bending mode at 540 cm^{-1} , are perhaps the most important features. That ν_3 is a result of a weak β CH bond and is not perturbed by any other modes was shown in a previous study on the HCD_2CD_2 isotope.⁸ This isotopic species contained only one absorption in the CH stretching region at 2840 cm^{-1} , and hence it was concluded that ν_3 was not perturbed by other vibrational modes in the system. Other studies²⁰ on the isopropyl, *tert*-butyl, *n*-propyl, *n*-butyl, and isobutyl radicals have amply demonstrated that this band is a characteristic feature of a weak CH bond β to a radical center. ν_9 is the most intense band in the infrared spectrum of the ethyl radical. A possible origin of the very large bandwidth for ν_9 is worthy of discussion. In Figure 10, two plots are shown. The first is for the changes in potential energy against α , the angle for internal rotation about the CC bond. Structures are drawn in the figure illustrating the orientation of the ethyl radical for

various values of α (in reality this sixfold potential function represents an energy path because the geometry is completely optimized for various values of α). Only very small changes in energy (≈ 150 cal) are required to convert from one minimum to another. The barrier is indeed small and infrared and ESR measurements are in agreement on this point.^{1,3,7} The second plot is for γ , the angle between the plane formed by the CH_2 group and the CC bond, against α . In essence, this plot expresses the geometric changes about the radical center as internal rotation proceeds. Note that when $\alpha = 0$, $\beta = 6^\circ$, the radical center is tilted toward the eclipsed β CH bond; when $\alpha = 30^\circ$, the system is at the top of a barrier and the radical center is planar, therefore, $\beta = 0$. Another 30° rotation to $\alpha = 60^\circ$ brings the system to another minimum, but the radical center must invert to $\beta \approx -6^\circ$. Consequently, in spite of the very low 150-cal barrier for internal rotation about the CC bond, rather dramatic geometric changes take place about the radical center. This could lead to a splitting of the bending mode (ν_9) via a coupled inversion-internal rotation motion if several levels exist below the barrier shown in Figure 10, or to a broadening if the levels are above the barrier; the latter case is a better description for the ethyl radical.

The symmetric and asymmetric stretching modes, ν_1 and ν_{10} , at 3033 and 3112 cm^{-1} reveal that the CH bonds α to the radical center are short ethylenic type bonds. Evidence for the decrease in the bond lengths α to a radical center is not only found in the CH stretching region but is also obtained by the high frequency for ν_7 , the CC stretching mode at 1175 cm^{-1} . In ethane, the CC stretch is about 150 cm^{-1} lower in frequency than that for the ethyl radical. This is a direct indication of the decrease in the CC bond length created by the unpaired electron. Theoretical results support this,¹² for example, the computed CC bond lengths for ethane and the ethyl radical are 1.528 and 1.498 \AA , respectively.

Summary

Extensive isotopic and theoretical studies have provided an assignment for the infrared spectrum of the ethyl radical. The vibrational modes that are a manifestation of the unpaired electron are a direct result of a weak CH bond β to the radical center, shorter than normal CH and CC bonds α to the radical center, and a methylene group that easily undergoes a pyramidal (umbrella) type motion. These coupled with a low barrier for internal rotation about the CC bond have created a very interesting spectrum for the ethyl radical.

Registry No. Ethane, 74-84-0; ethylene, 74-85-1; dipropionyl peroxide, 3248-28-0; butane, 106-97-8; CH_3CH_2 , 2025-56-1; CH_3CD_2 , 28882-22-6; CD_3CH_2 , 61307-92-4; CD_3CD_2 , 71668-46-7; $\text{CH}_3\text{CD}_2\text{CO}_2\text{O}_2\text{CCD}_2\text{CH}_3$, 79898-68-3; $\text{CD}_3\text{CH}_2\text{CO}_2\text{O}_2\text{CCH}_2\text{CD}_3$, 79898-69-4; $\text{CD}_3\text{CD}_2\text{CO}_2\text{O}_2\text{C}-\text{CD}_2\text{CD}_3$, 79898-70-7.

(20) J. Pacansky, D. W. Brown, and J. S. Chang, *J. Phys. Chem.* **85**, 2562 (1981).